

AD-A132 743

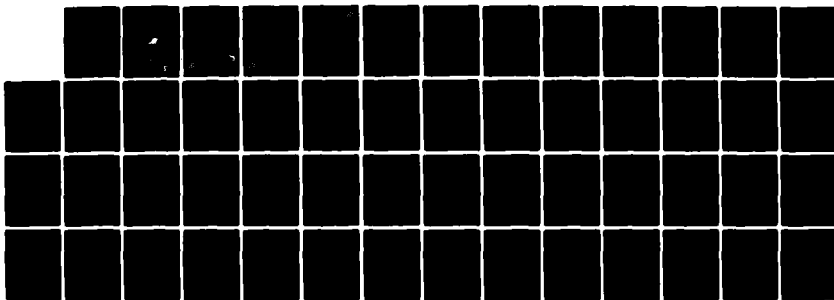
HIGH POWER RARE GAS HALIDE LASER(U) SCIENCE
APPLICATIONS INC MCLEAN VA T G FINN ET AL. 07 MAR 79
SAI-164-068-250 N00173-78-C-0414

1/1

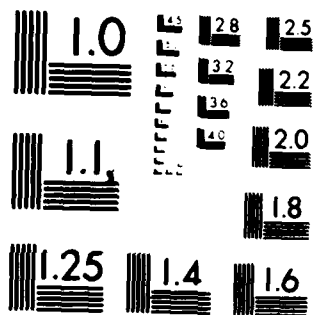
UNCLASSIFIED

F/G 20/5

NL



END
DATE
FILMED
10-83
DTIC



MICROCOPY RESOLUTION TEST CHART
NATIONAL BUREAU OF STANDARDS-1963-A

AD-A132 743

①

File



APPROVED FOR PUBLIC RELEASE
DISTRIBUTION UNLIMITED

SCIENCE APPLICATIONS, INC.

DTIC FILE COPY

DTIC
SELECTED
SEP 21 1983

A
88 09 20 185

1

HIGH POWER RARE GAS
HALIDE LASER

Final Report

164-068-250

APPROVED FOR PUBLIC RELEASE
DISTRIBUTION UNLIMITED



ATLANTA • ANN ARBOR • BOSTON • CHICAGO • CLEVELAND • DENVER • HUNTSVILLE • LA JOLLA
LITTLE ROCK • LOS ANGELES • SAN FRANCISCO • SANTA BARBARA • TUCSON • WASHINGTON

DTIC
SELECT
SEP 21 1983
A

HIGH POWER RARE GAS
HALIDE LASER

Final Report

APPROVED FOR
DISTRIBUTION USE

SAI 164-068-250

T. G. Finn

L. J. Palumbo (NRL)

L. F. Champagne (NRL)

NRL 5540-52:TGF/LJP:rmb



ATLANTA • ANN ARBOR • BOSTON • CHICAGO • CLEVELAND • DENVER • HUNTSVILLE • LA JOLLA
LITTLE ROCK • LOS ANGELES • SAN FRANCISCO • SANTA BARBARA • TUCSON • WASHINGTON



7 March 1979

Director
Naval Research Laboratory
4555 Overlook Avenue, S.W.
Washington, D. C. 20375

Attn: Dr. W. Watt, Code 5540

Reference: Contract No. N00173-78-C-0414

Subject: Contract Data Requirement A001 per DD1423

Dear Dr. Watt:

Enclosed are three (3) copies each of the subject report in accordance with the requirements of the referenced contract.

Very truly yours,

SCIENCE APPLICATIONS, INCORPORATED

Thomas Finn

Thomas Finn
Project Scientist

TF:km
Enc.

APPROVED FOR PUBLIC RELEASE
DISTRIBUTION UNLIMITED

Science Applications, Inc. 3400 Westpark Drive, McLean, Virginia 22101, (703) 821-4300

SAI Offices: Albuquerque, Ann Arbor, Arlington, Atlanta, Boston, Chicago, Huntsville, La Jolla, Los Angeles, Palo Alto, Santa Barbara, Sunnyvale, and Tucson.

HIGH POWER RARE GAS
HALIDE LASER

March 1979

Final Report

164-068-250

Prepared for:

Naval Research Laboratory
4555 Overlook Avenue, S. W.
Washington, D. C. 20375

APPROVED FOR PUBLIC RELEASE
DISTRIBUTION UNLIMITED

SCIENCE APPLICATIONS, INCORPORATED

8400 Westpark Drive, McLean, Virginia 22102
(703) 821-4300



APPROVED FOR PUBLIC RELEASE	
DISTRIBUTION UNLIMITED	
164-068-250	
March 1979	
Final Report	
HIGH POWER RARE GAS HALIDE LASER	
Prepared for: Naval Research Laboratory 4555 Overlook Avenue, S. W. Washington, D. C. 20375	
SCIENCE APPLICATIONS, INCORPORATED 8400 Westpark Drive, McLean, Virginia 22102 (703) 821-4300	
Doc A	

TABLE OF CONTENTS

	<u>Page</u>
I. INTRODUCTION	1
II. APPARATUS	2
III. XeF INVESTIGATIONS	4
IV. XeCl INVESTIGATIONS	7
V. APPENDIX	

Section I

INTRODUCTION

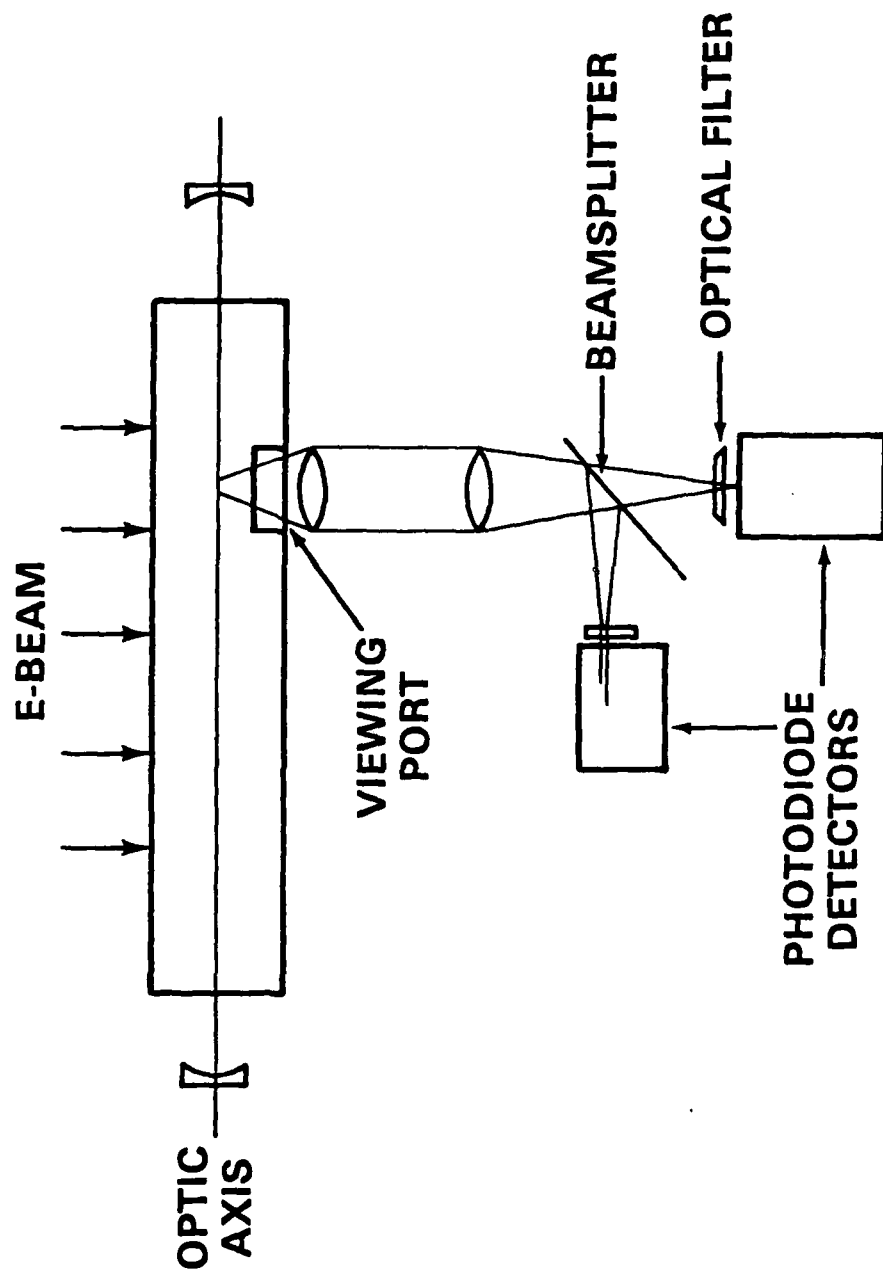
During the course of this contract, solid progress was made in both the development and understanding of rare gas halide lasers. Initially, to comprehend the major processes which occur in the laser plasma, we developed a long pulse kinetics experiment which simulated closely the laser kinetics. The experiment was used to investigate the kinetics of the XeF laser and, later, the XeCl laser, both with neon as a diluent. In general, the experiment provided information on the fluorescence yield, the formation efficiency and the apparent quenching rate constants for the upper laser level. For XeF, the results of the experiment served as a basis for a computer code which simulated long pulse operation of the XeF laser. The code was used to investigate various processes in the laser such as formation, absorption and ground state bottlenecking. The role of the XeF(C) was unraveled using the model, and, also the effects of halogen donor depletion. For XeCl, the experiment has provided information on the fluorescence yield and apparent quenching rate constants for the XeCl(B) state. Preliminary modeling analysis of XeCl indicates that the formation efficiency is close to 100 percent.—

Section II

APPARATUS

The apparatus consists of a kinetics chamber which is mounted onto a cold-cathode electron beam chamber. The kinetics chamber is made from aluminum and has an active volume of $1.5 \times 20 \text{ cm}^3$. The chamber is mounted directly to the electron gun vacuum chamber with a thin titanium foil separating the two. The cold-cathode electron gun produces a beam of 280 KeV electrons with a pulse duration of 1 usec. The peak current density into the laser gas is 2 A/cm^2 . Fluorescence is observed perpendicular or parallel to the electron beam direction with calibrated photodiodes and filters. A diagram of the apparatus is shown in Figure 1. The dominant kinetic processes have characteristic times which are much shorter than the pulse duration, thus the excited and ionic species are in quasi-equilibrium.

KINETICS EXPERIMENT



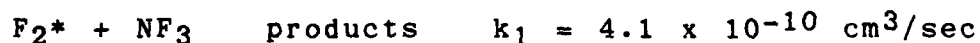
ACTIVE VOLUME: 20 cm x 1 cm x 1 cm

Figure 1. A schematic diagram of the long pulse kinetics experiment.

Section III

XeF INVESTIGATIONS

With the kinetics experiment we were able to characterize the fluorescence from the B & C states of XeF and measure the apparent quenching rates. The results indicate that almost all the excitation is channeled through the XeF molecule, and that approximately 80 percent finds itself in the B state. The apparent quenching rate constants for neon and xenon are in good agreement with the actual quenching rate constants obtained by other methods. The agreement indicates that interception by the rare gases is not significant. On the other hand, the apparent rate constant for NF₃ was much larger than the actual value. We attribute this difference to interception in the XeF formation chain by NF₃. The magnitude of the interception effect correlates with the process:



which has been proposed by Heustis (1). The apparent quenching rates for XeF(B) are given in Table I.

The experimental results were used to develop a model which simulates the XeF laser in a neon diluent. The code has provided a wealth of information on how the laser works and its limitations. First, the model determined the formation chain of the laser upper level, the XeF(B) state, in particular, it illuminated the importance of the neutral formation which proceeds through the

mechanism of Penning ionization. Second, the model calculated the maximum efficiency which the laser could achieve; this value is close to the efficiency corresponding to one laser photon per ion formed (10 percent). Third, the model was used to investigate absorption at the laser wavelength in the laser mix and in corresponding rare gas mixtures. The model determined that in pure neon there is a strong absorption due to excited neutral neon which is removed by the addition of a small amount of xenon. However, in the laser mix absorption is dominated by Xe_2^+ and this process limits the amount of xenon which can be added to it. Fourth, the model was employed to investigate the effect of the weakly bound XeF ground state. The model predicted that the laser performance would improve if the ground state was removed more rapidly as through heating. A preprint of the model results is included. The model results have been published (2).

The computer code was used to determine the role of the $\text{XeF}(\text{C})$ in laser performance. The C state, which emits in a broad band centered around 460 nm, is important because in the laser mix 40 percent of the total emission is from this state. If this emission represents a process which intercepts formation of the laser upper level, then the ultimate efficiency of the XeF laser is substantially limited. If, on the other hand, the C state is formed through the B state then other processes limit the efficiency of the laser. A model was constructed based on neutral kinetics as experimental evidence indicated that electron mixing was not significant. The model predicted

the following results. First, two thirds of the C state population is formed from quenching of the B state. In addition, 25 percent of the excitation which forms the B state goes directly into the C state. Third, the quenching rates for the C state are much less than those for the B state. From the model, we conclude that the enhanced C emission does not result from interception of the B state, but rather is due to quenching from B to C and less quenching of the C state by the diluent. Thus the model indicates that other processes such as vibrational relaxation or ground state absorption limit the laser efficiency. A preprint of the C state results is included. The results have been published (3).

The model was used to study depletion of the NF_3 halogen donor in the XeF laser. If the E-beam pumping pulse is extended beyond 1 usec, significant depletion of the halogen donor can occur. The extent of depletion depends primarily on the termolecular recombination rate which controls NF_3 reformation. The effect of depletion depends on the electron attachment rates of the depletion products which control the F^- production. The two major effects of depletion are increased absorption due to Xe_2^+ , and increased formation through the Xe^* neutral reactions. A technical memorandum based on the results of the depletion study is enclosed.

Section IV

XeCl INVESTIGATIONS

XeCl in a neon diluent has exhibited 5 percent efficiency and is of great interest to the Navy as it can be shifted into the blue-green region of the spectrum. Our approach has been twofold - experimental and theoretical. In the kinetics experiment, we have measured the fluorescence efficiency of the B state, and the apparent quenching rate constants for neon, xenon and HCl. In Table I, the rates are given and compared to the values obtained for XeF. As one can see, the XeCl rate constants are lower than the XeF values, and partly for this reason, XeCl has a higher fluorescence efficiency. Furthermore, the rate constant for HCl is abnormally large which could indicate some intercept by the halogen donor. A similar situation exists for NF₃.

Modeling analysis of rare gas mixtures has shed some light on the major absorption species at the laser wavelength. The model shows that the absorber in pure neon is Ne₂* which is removed dramatically by the addition of xenon to the mixture. Furthermore, the amount of additional xenon is ultimately limited by its contribution to absorption. In Figures 2 through 4, we show the model predictions for the density of species in neon and neon/xenon mixtures. In Figure 2, we see that only Ne₂* can explain the rapid drop off in absorption when xenon is added. In Figure 3, we see further that the flat appearance of the absorption curve correlates strongly with the

Xe₂⁺ density. Moreover, in Figure 4, we see that at xenon concentrations of 2 percent or more, absorption by Xe₂⁺ or Xe₃⁺ appears to become significant. As a final point, in Table II, we summarize the energy efficiencies of XeCl which we derive from a combination of experiment and model.

REFERENCES

1. Heustis et al., J. Chem. Phys. 69, 5133 (1978).
2. Finn, Palumbo, Champagne, Appl. Phys. Lett. 33, 148 (1978).
3. Finn, Palumbo, Champagne, Appl. Phys. Lett. 34, 52 (1979).

Table I
Apparent Quenching Rate Constants

	<u>XeCl₂ (B)</u>	<u>XeF (B)</u>
Ne	5.3×10^{-13}	9.3×10^{-13}
Ne + 1% Xe		
Ne + Ne	$< 2 \times 10^{-34}$	2.8×10^{-33}
Xe	7.8×10^{-12}	7.3×10^{-11}
Halogen Donor	5.5×10^{-10}	6.8×10^{-10}
Fluorescence Efficiency (Per Ion Pair)	50%	50%

Table II
Energy Efficiency of XeCl

Formation	$11 \pm 2\%$	Experiment and Model
Fluorescence	$5 \pm 1\%$	Experiment
Extraction	$5 \pm 1\%$	Model

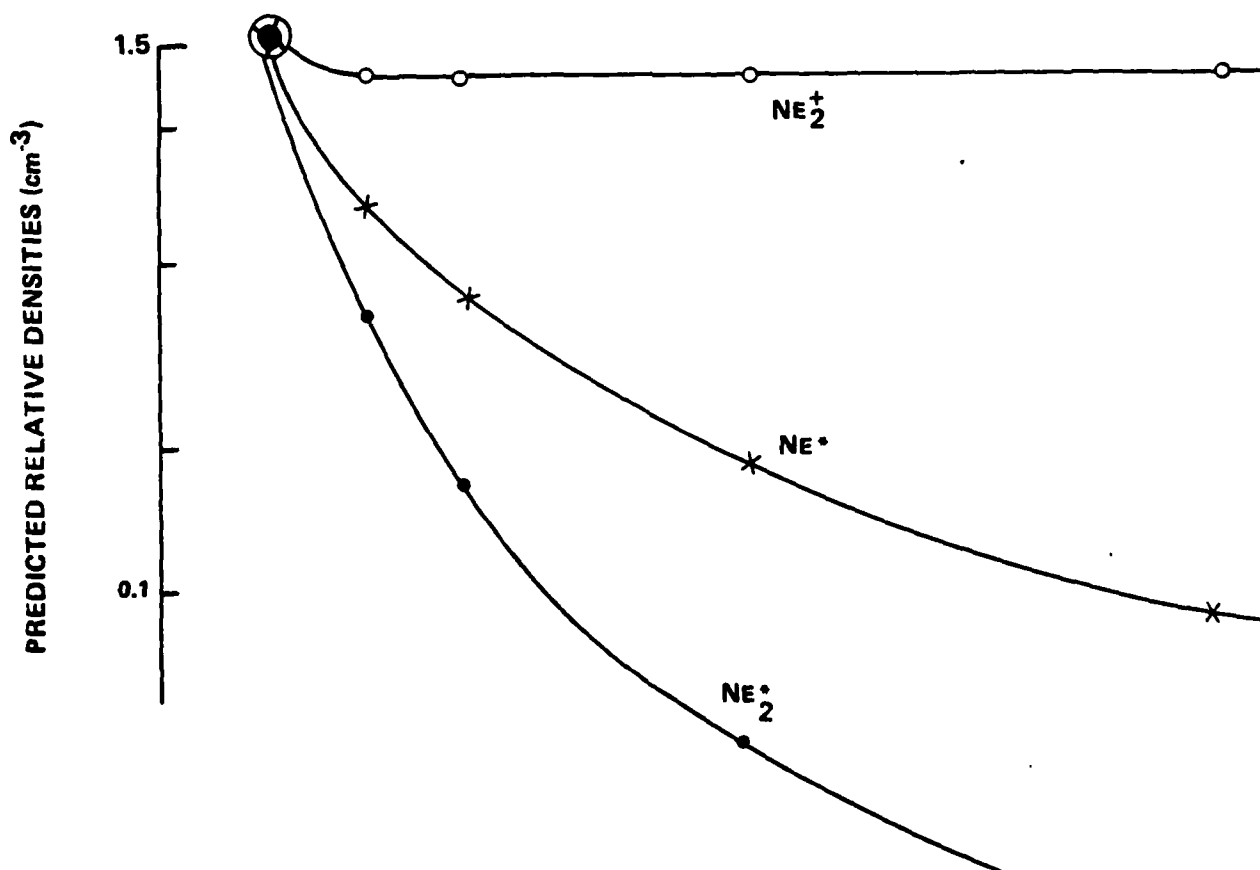
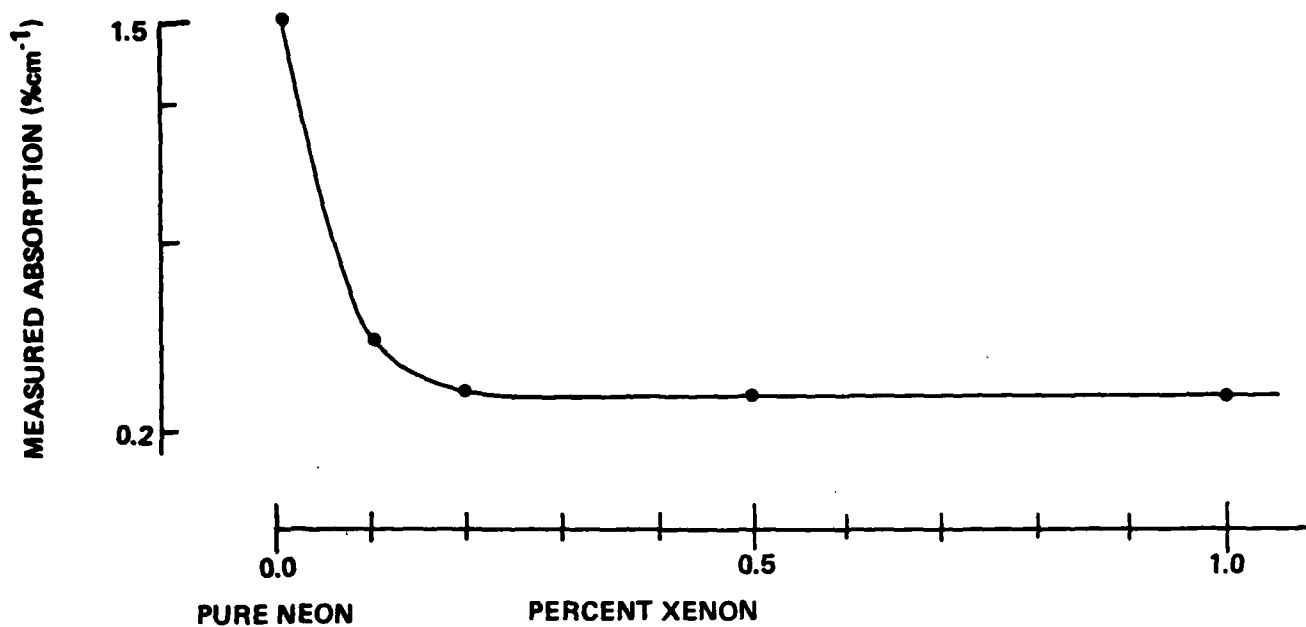


Figure 2. Top: Measured absorption at 308 nm in pure neon, and neon/xenon mixtures.
Bottom: Model prediction of densities of neon excited species.

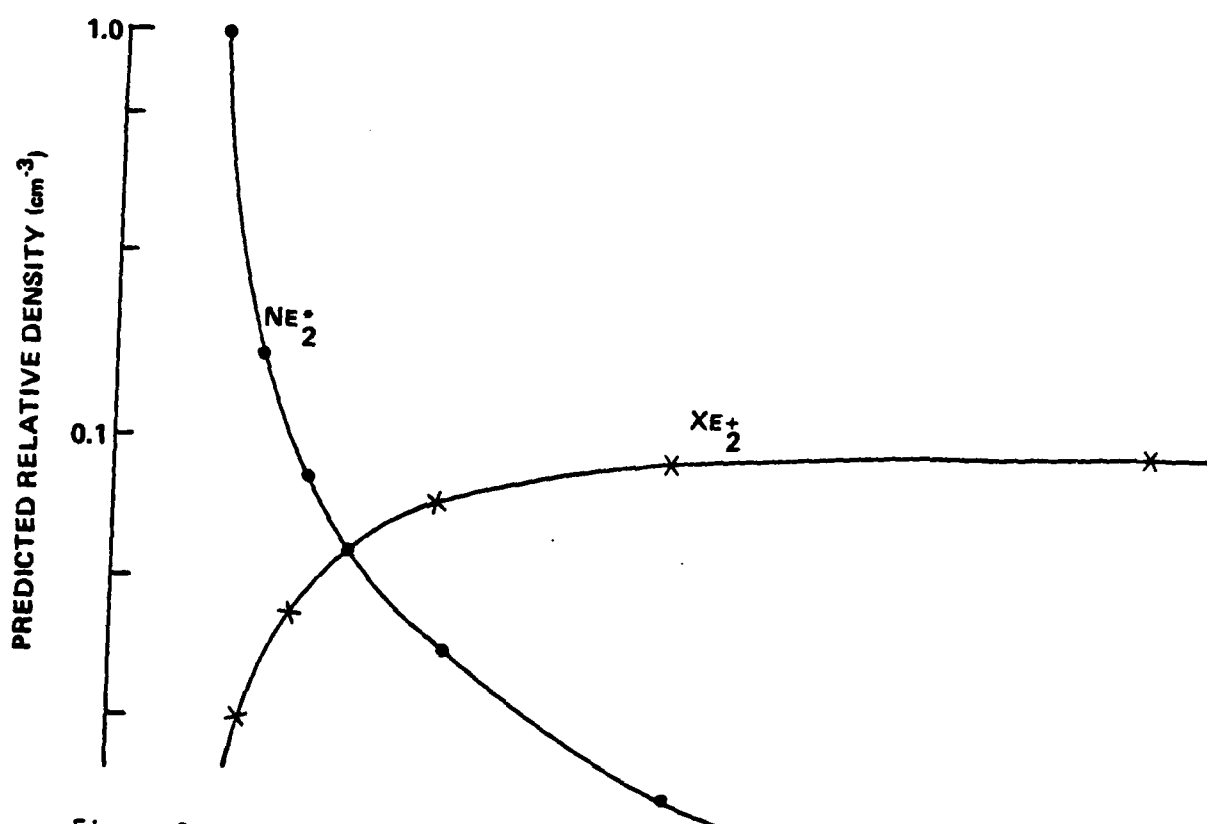
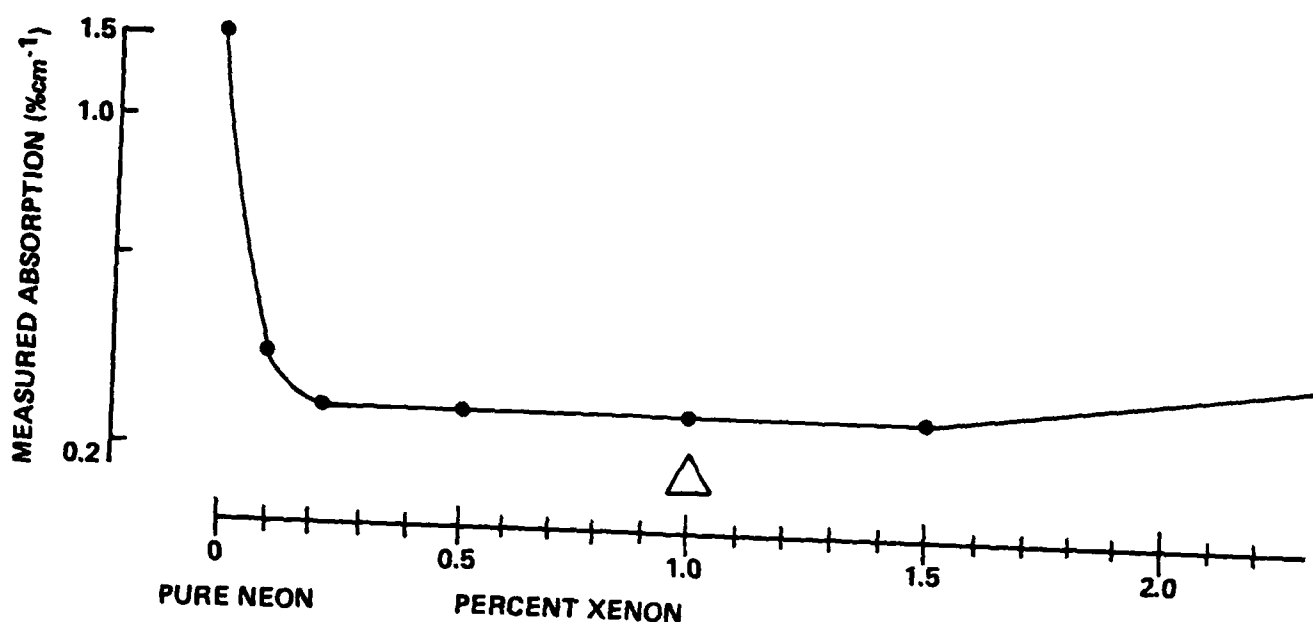


Figure 3. Top: Measured absorption at 308 nm in pure neon, and neon/xenon mixtures.
Bottom: Model prediction of densities of Ne_2^+ and Xe_2^+ .

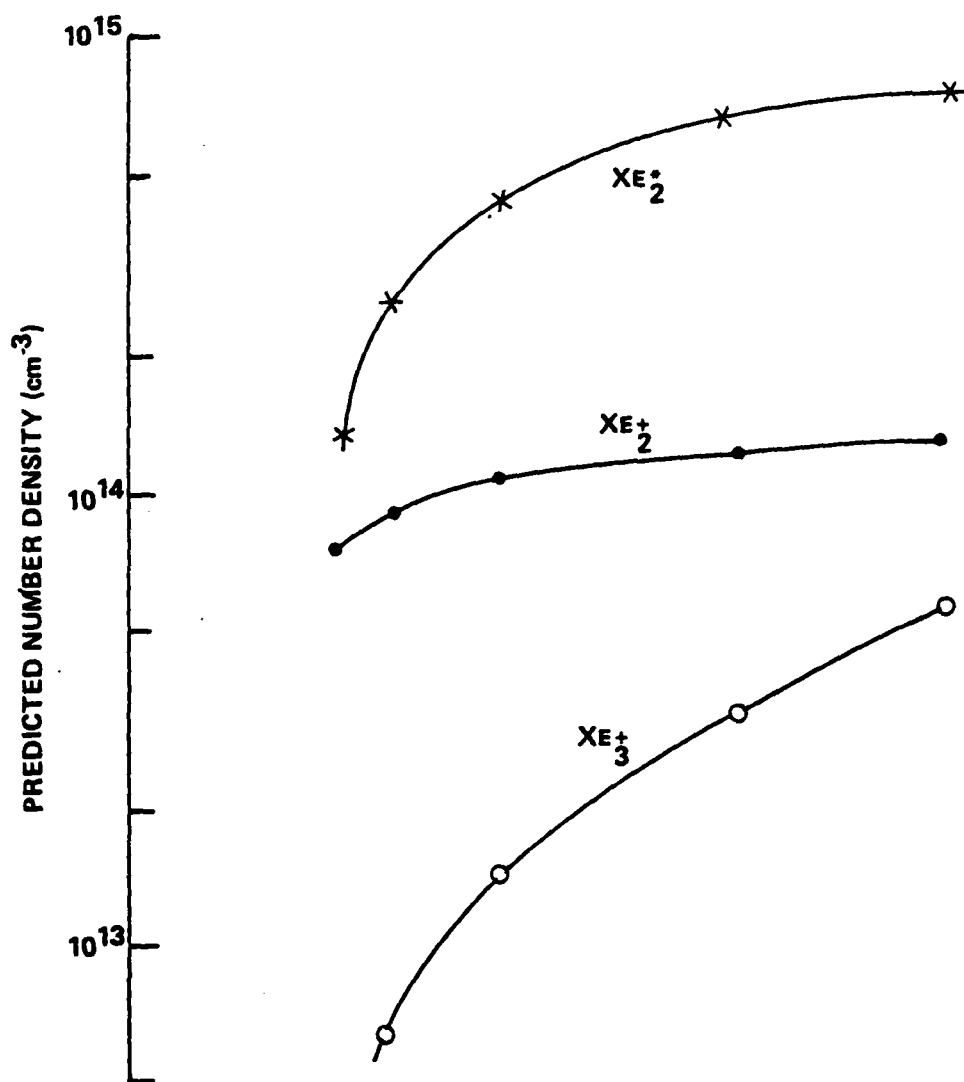
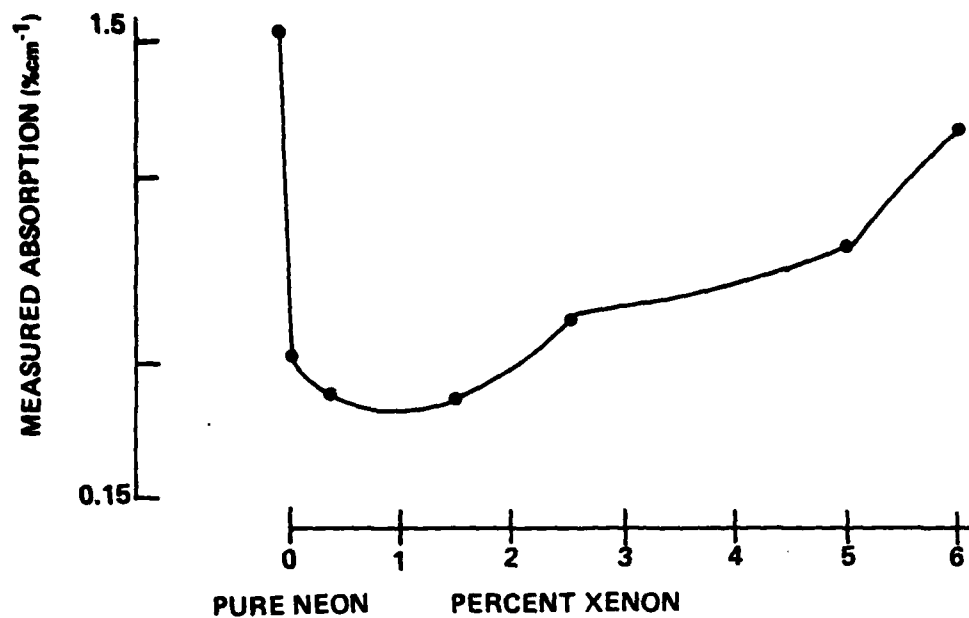


Figure 4. Top: Measured absorption at 308 nm in pure neon, and neon/xenon mixtures. Bottom: Model prediction of densities of excited xenon species.

A KINETICS SCHEME FOR THE XeF LASER

T. G. Finn,* L. J. Palumbo, and L. F. Champagne
Laser Physics Branch
Optical Sciences Division
Naval Research Laboratory
Washington, D. C. 20375

ABSTRACT

A kinetics scheme is described for electron-beam excitation of the XeF laser in a neon diluent. Both Ne^+ and Ne^* channels contribute significantly to the formation of the upper laser level. In each chain an important Penning ionization process leads to the formation of Xe^+ , which is the major intermediary in forming the upper laser level. Xe_2^+ is found to be the dominant absorber of laser radiation. The effect of the weakly bound XeF ground state is discussed.

* Science Applications, Inc., Arlington, VA 22015

Since the first demonstration of exciplex fluorescence in rare gas halide systems,¹ there has been considerable interest in developing these systems into efficient and powerful UV lasers.² Recent work at NRL has demonstrated efficient and powerful XeF laser operation in a neon diluent.³ However, a thorough understanding of the laser kinetics is necessary in order to project the maximum efficiency of this system. This paper reports a kinetics scheme by which energy deposited by an electron-beam is channeled into the upper laser level and is ultimately extracted. The scheme is derived from a computer simulation of an E-beam pumped XeF laser operating at optimum experimental conditions. Processes which limit laser performance are discussed.

The computer model consists of two parts: first, an E-beam deposition section, in which the kinetic energy of near relativistic electrons is used to ionize and excite the laser gas, and second, a chemical kinetics section, in which the energy deposited in the gas cascades down by various processes to the upper laser level and is extracted as laser radiation.

The energy deposited by the E-beam in the laser mixture is calculated using a high energy electron deposition computer code⁴ based on the work of Berger and Seltzer.⁵ Because the target gas is not "thin", the electrons traverse in a zig-zag path which results in greater energy deposition. The total deposition for our device has been calculated to be approximately two and one-half times the Berger and Seltzer values, and has been verified experimentally by nitrous oxide dosimetry.

The second part of the computer code deals with kinetics. In this

section chemical reactions transport the deposited energy along various competing channels, some of which lead to the upper laser level. The dominant chains are determined by following the excitation which is deposited initially in Ne^+ and Ne^* as it travels from species to species and eventually reaches the upper laser level or some other species. For example, our model indicates that when the excitation reaches Ne_2^+ this ion is five times more likely to recombine with F^- to form NeF^* than with electrons to form Ne^* . Hence the dominant path leads from Ne_2^+ to NeF^* and so forth until it reaches the upper laser level or a species which is unlikely to form the upper laser level. The model does not consider the internal structure of the XeF^* molecules, that is, the role of the $\text{XeF}(\text{C})$ state and vibrational relaxation of the B state. However, these effects are taken into account in estimating the overall efficiency of the system. Many of the chemical reaction rates have been measured but several have only been calculated or at best estimated. For example, recombination reactions of the form $\text{M}^+ + \text{F}^-$, where M^+ is a rare gas atomic or molecular ion, have been calculated to reach a maximum of approximately $2-3 \times 10^{-6} \text{ cm}^3/\text{sec}$ at a few atmospheres of pressure, and then to drop off linearly with increasing pressure.⁶ Consequently, for these reactions, we assumed a reaction rate of $1 \times 10^{-6} \text{ cm}^3/\text{sec}$ at our operating conditions of five atmospheres. For electron dissociative attachment of the fluorine donor we assumed a rate of $1 \times 10^{-9} \text{ cm}^3/\text{sec}$.

In the Ne/Xe/NF_3 laser, energy is channeled into the upper laser level primarily through the mechanism of Penning ionization. Both ion and neutral channels contribute significantly. In each chain an important Penning step leads to the formation of Xe^+ , which is the primary intermediary in forming the laser upper level. The major kinetics chains are represented in Fig. 1.

Most of the excitation energy results in forming Ne^+ which, either directly or through complex ion species, reacts with F^- to form NeF^* . The NeF^* molecule rapidly predissociates to form F^* which ionizes Xe^7 . This Penning reaction is the major source of Xe^+ , which can form the upper laser level through its recombination with F^- . The major loss mechanism in this chain is quenching of F^* by NF_3 . Although excited NF_3 has enough internal energy to react with Xe and form the upper laser level, this reaction has yet to be demonstrated. A significant fraction of the energy deposited produces Ne^* which directly or through complex molecules forms Xe^+ by a Penning reaction. Emission from the Ne_2^* excimer is an apparent loss process from this chain but this radiation has sufficient energy to ionize Xe and thus constitutes an additional formation channel.

Almost all of the excitation energy which reaches the upper laser level travels through Xe^+ which forms XeF^* by recombination with F^- . However, we speculate that at high pressure Xe^+ forms the weakly bound complex, NeXe^+ . Little is known of NeXe^+ except that it has an emission spectrum.⁸ If NeXe^+ is formed, it rapidly forms the upper laser level directly through recombination with F^- or indirectly through another species such as Xe_2^+ or Xe^* , which is formed from dissociative recombination of NeXe^+ or Xe_2^+ . In any case once the excitation reaches Xe^+ it is rapidly channeled into XeF^* . Under the experimental conditions which the computer model simulated,³ and which are given in Fig. 1, 44% of all the excitation which reaches the upper laser level is extracted as laser output, 13% is absorbed (principally by Xe_2^+), 26% is quenched (principally by Ne), and 17% is lost through fluorescence.

Recently Rokni et al⁹ have investigated formation and quenching processes in Ne/Xe/F₂ mixtures and their results are in substantial agreement with the predictions of our model. However, in our model we have used NF₃ rather than F₂ as the fluorine donor because its use significantly increases the laser performance.¹⁰ Moreover, NF₃ quenches XeF* much less rapidly than F₂¹⁴ so that the major quenching species of XeF* is neon in our model rather than the fluorine donor as in Rokni's case. As a final point, Rokni et al show as a minor formation channel the reaction of F* with F₂ to produce F₂* which can react with Xe to form XeF*. Unfortunately, the equivalent formation process with NF₃ has yet to be demonstrated hence in our model we are compelled to treat it as an interception process.

The estimate of the overall energy efficiency is uncertain to the extent that the products of the complex ion recombination reaction with F⁻ are unknown as are the fate of these products. It has been generally accepted but not conclusively demonstrated that the upper laser level is formed with near unit efficiency as a product of the Xe⁺ and F⁻ recombination reaction. In addition, recent experiments on KrF formation in argon diluent indicate that in Kr₂⁺ recombination reactions, the product yield of KrF* is high.¹¹ However, not much is known of the reaction products of the complex ions, NeXe⁺ and Xe₂⁺. It is possible that a substantial amount of excitation is channeled into the XeF(C) state which may not rapidly couple to the B state, or the excitation may be channeled into high vibrational levels of the B state which do not relax to the laser level. At this stage much work needs to be done on the excited states of XeF. To account for the uncertainty in the yields of these complex ions, we have calculated the laser efficiency assuming product yields of unity for one case, and one fifth for the other.

Under these conditions, the energy efficiency for formation of XeF^* is 9% for the unity case and 5% for the one fifth case, likewise, the extraction efficiencies are 4% and 2%, respectively.

XeF has a weakly bound ground state which acts to trap the laser radiation and thus decrease the laser output. The ground state has a total well depth of 1100 cm^{-1} and a depth of approximately 800 cm^{-1} from the lower laser level.¹² The laser radiation is absorbed by the ground state and is rapidly re-stimulated. The result of this "recycling" of the laser radiation is that the net stimulated emission rate is decreased and, consequently, more excitation is lost through fluorescence and quenching. Collision with neon atoms can break apart the XeF ground state and thus increase the laser output. In Fig. 2, the laser efficiency is given as a function of the ground state removal rate. It is found that a dissociation rate constant of $3 \times 10^{-12} \text{ cm}^3/\text{sec}$ which corresponds to one half the gas kinetic rate and a well depth of 800 cm^{-1} fits the observed efficiency of 2.0%.³ Heating the laser gas to 600°K would increase the break apart by an order of magnitude and the laser efficiency by 50% as can be seen in the figure. However, we have not considered the effect of increased temperature on other aspects of the kinetics scheme such as formation, quenching and absorption.

When neon is substituted for argon as the diluent in the XeF laser, a significant improvement in laser performance is observed which is due to the decrease in the transient absorption.³ Recent theoretical predictions of the absorption spectra of rare gas dimers indicate that Ar_2^+ absorbs in the 350 nm region, whereas Ne_2^+ does not.¹³ In order to determine what species is responsible for the remaining absorption in the XeF laser, we compared to our kinetic model the results of several previous absorption

experiments conducted in pure rare gas mixtures and the laser mixture.³

In Fig. 3 the observed absorption as a function of gas composition is compared to the relative densities predicted by the model.

In the first experiment, conducted in pure neon, we observed an absorption of 1.25%/cm which decreased to 0.2%/cm when 0.1% Xe was added to the mixture. Looking at the lower half of Fig. 3, we note that the only species that decreases significantly when Xe is added is Ne_2^* , hence Ne_2^* is most likely the major absorber in pure neon plasmas. When the Xe concentration is increased to 1%, as in experiment three (Fig. 3), the absorption increases to 1.25%/cm. However, we note that the density of the excited neon species has decreased while the density of Xe_2^+ and Xe_2^* have increased as has the absorption. In the final experiment, performed on the laser mixture, we note that the absorption has decreased significantly as have the Xe_2^+ and Xe_2^* densities. By combining the theoretical estimate¹³ of the absorption cross section at the laser wavelength of Xe_2^+ with the model prediction of its density, we can calculate the absorption in the laser mixture due to Xe_2^+ , and this value, given by the "X" in Fig. 3, is in good agreement with the observed value. The evidence clearly points to Xe_2^+ as the dominant absorber.

In the XeF laser when neon is the diluent the dominant process for formation of the upper laser level is Penning ionization, a channel which does not exist in argon diluent. Because of the high operating pressure of this laser, a significant role is played by complex and poorly understood species such as NeXe^+ . An increase in the laser output of approximately 50% can be obtained by more effective removal of the XeF ground state. Use

of neon as a diluent eliminates the transient absorption at the laser wavelength which exists in an argon diluent, however, under optimum laser conditions the major absorber is Xe_2^+ .

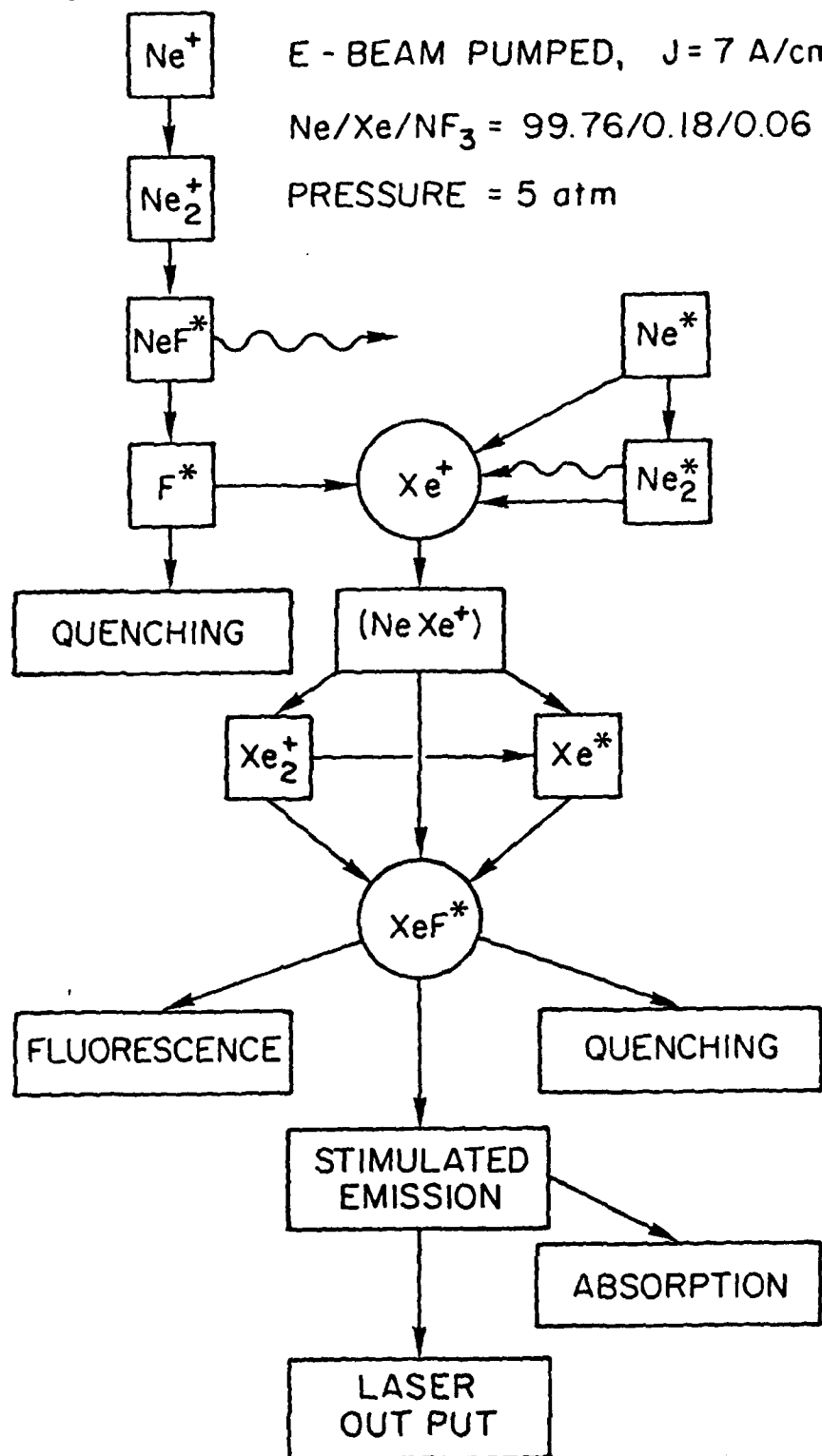
We wish to thank D. L. Huestis, SRI, for making available to us his unpublished data, and for helpful conversations.

REFERENCES

1. M. F. Golde and B. A. Thrush, Chem. Phys. Lett. 29, 486 (1974);
J. E. Velazco and D. W. Setser, J. Chem. Phys. 62, 1990 (1975).
2. S. K. Searles and G. A. Hart, Appl. Phys. Lett. 27, 243 (1975); J. J. Ewing and C. A. Brau, Appl. Phys. Lett. 27, 350 (1975); E. R. Ault, R. S. Bradford, And M. L. Bhaumik, Appl. Phys. Lett. 27, 413 (1975).
3. a) L. F. Champagne, J. G. Eden, N. W. Harris, N. Djeu and S. K. Searles, Appl. Phys. Lett. 30, 160 (1977).
b) L. F. Champagne and N. W. Harris, Appl. Phys. Lett. 31, 513 (1977).
c) L. F. Champagne, "The Influence of Diluent Gas on the Xenon Fluoride Laser," Electronic Transition Lasers III, ed. by K. L. Kampa and H. Walther (Springer-Verlag, Berlin) 1978, p. 32.
4. D. B. Brown, D. B. Wittry and D. F. Kyser, J. Appl. Phys. 40, 1627 (1969).
5. M. J. Berger and S. M. Seltzer, "Tables of Losses and Ranges of Electrons and Positrons," NASA Report No. SP-3012 (1964).
6. J. M. Wadehra and J. N. Bardsley, Appl. Phys. Lett. 32, 76 (1978).
7. N. W. Winter, C. F. Bender and T. N. Rescigno, J. Chem. Phys. 67, 3122 (1977).
8. Y. Tanaka, K. Yoshino and D.E. Freeman, J. Chem. Phys. 62, 4488 (1975).
9. M. Rokni, J. H. Jacob, J. A. Mangano and R. Brochu, Appl. Phys. Lett. 32, 223 (1978).
10. L. F. Champagne (unpublished).
11. M. Rokni, J. H. Jacob and J. A. Mangano, Phys. Rev. A 16, 2216 (1977).
12. J. Tellinghuisen, G. C. Tisone, J. M. Hoffman and A. K. Hays, J. Chem. Phys. 64, 4796 (1976).
13. W. Wadt, D. C. Cartwright and J. S. Cohen, Appl. Phys. Lett. 31, 673 (1977).
14. H. C. Brashears, Jr., D. W. Setser and D. DesMarteau, Chem. Phys. Lett. 48, 84 (1977).

FIGURE CAPTIONS

1. Kinetics scheme for E-beam pumped XeF laser in neon diluent. The species NeXe^+ is in parenthesis to denote that its presence is speculative. The operating pressure is five atmospheres.
2. Laser efficiency as a function of the XeF ground state dissociation rate. A rate constant of $3 \times 10^{-12} \text{ cm}^3/\text{sec}$ agrees with the experimental efficiency result of 2.0%. Increasing the gas temperature to 600°K should increase the laser efficiency significantly.
3. Top: Experimentally observed transient absorption at 351 nm in various gas mixtures; Bottom: Model calculations of the relative density of various species. The absorption decrease in neon when .1% xenon is added correlates with the decrease in the Ne_2^* density. The increased absorption in 1% xenon and subsequent decrease in the laser mix correlates with the Xe_2^+ and Xe_2^* densities. The "X" in the top figure is the Xe_2^+ absorption in the laser mixture calculated using the cross section of Reference (13). Note that this quantity can explain the observed absorption.



PARAMETER STUDY OF XeF(X) DEACTIVATION .

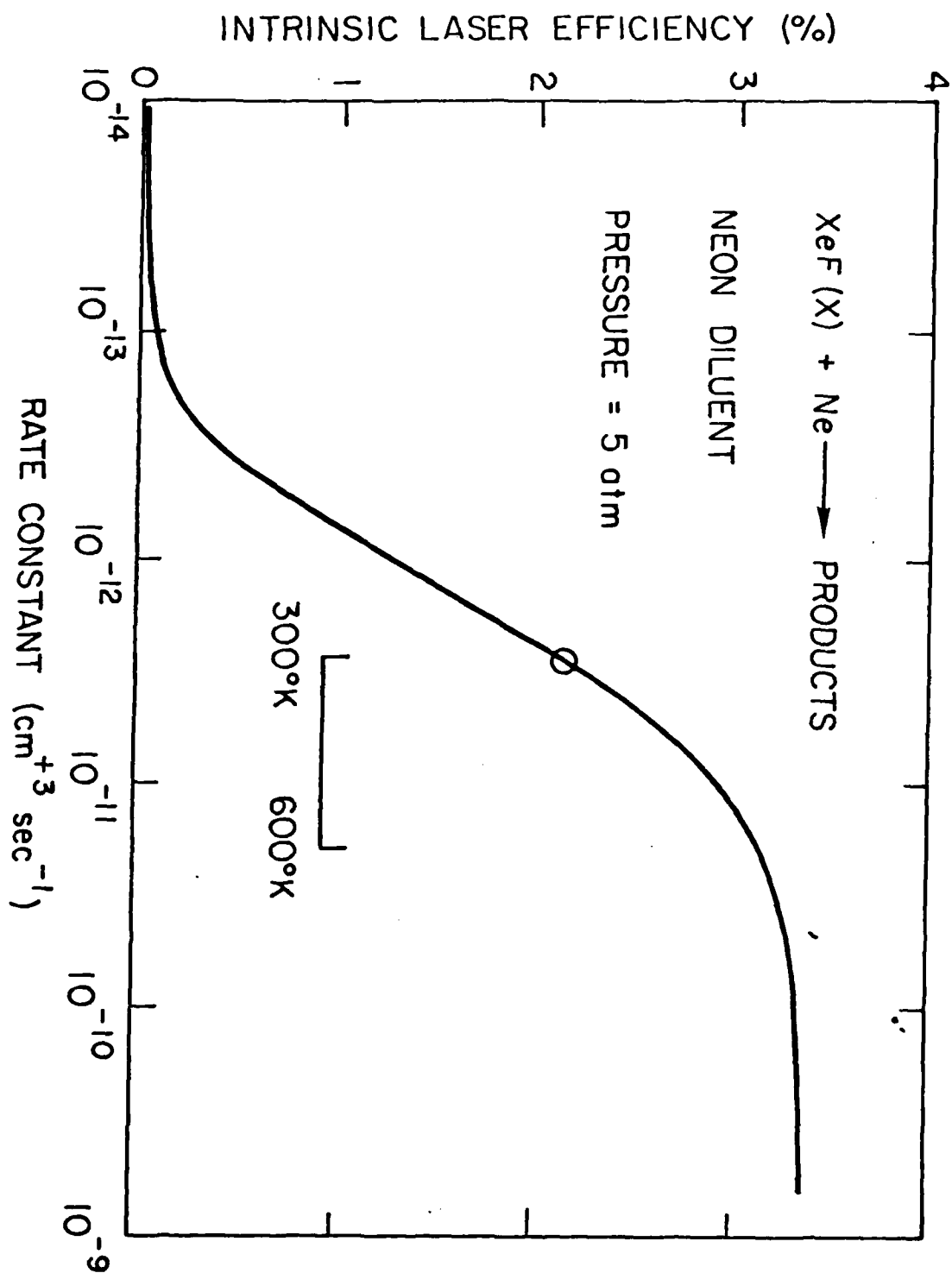


Fig. 2

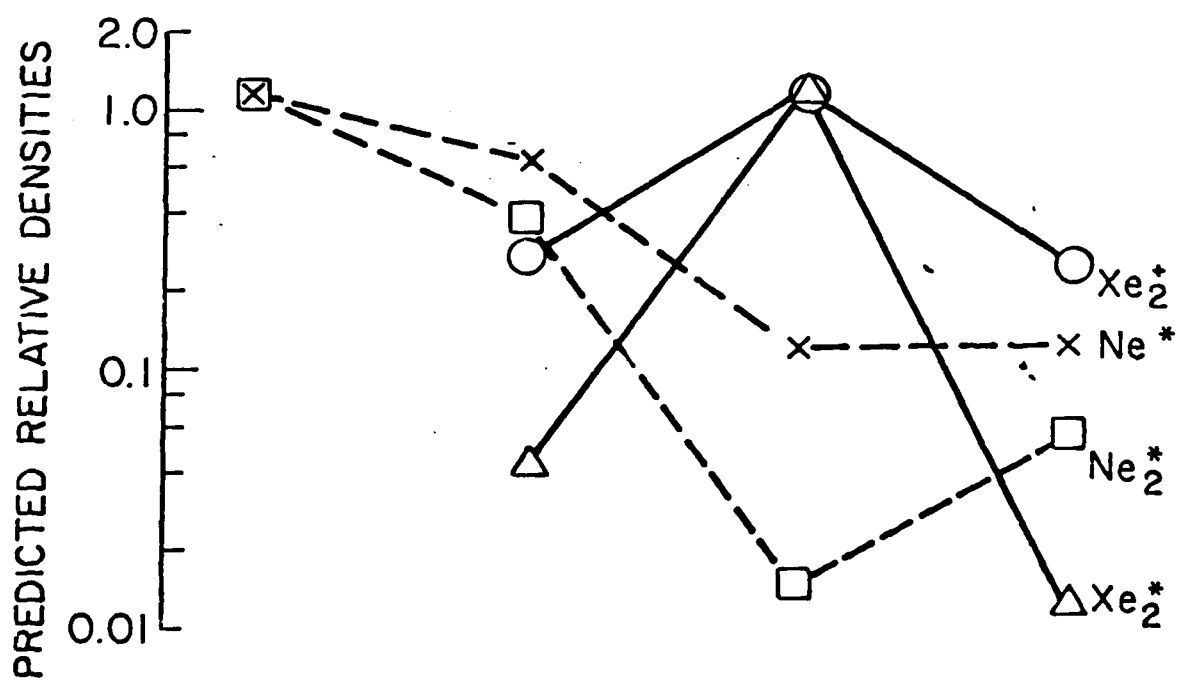
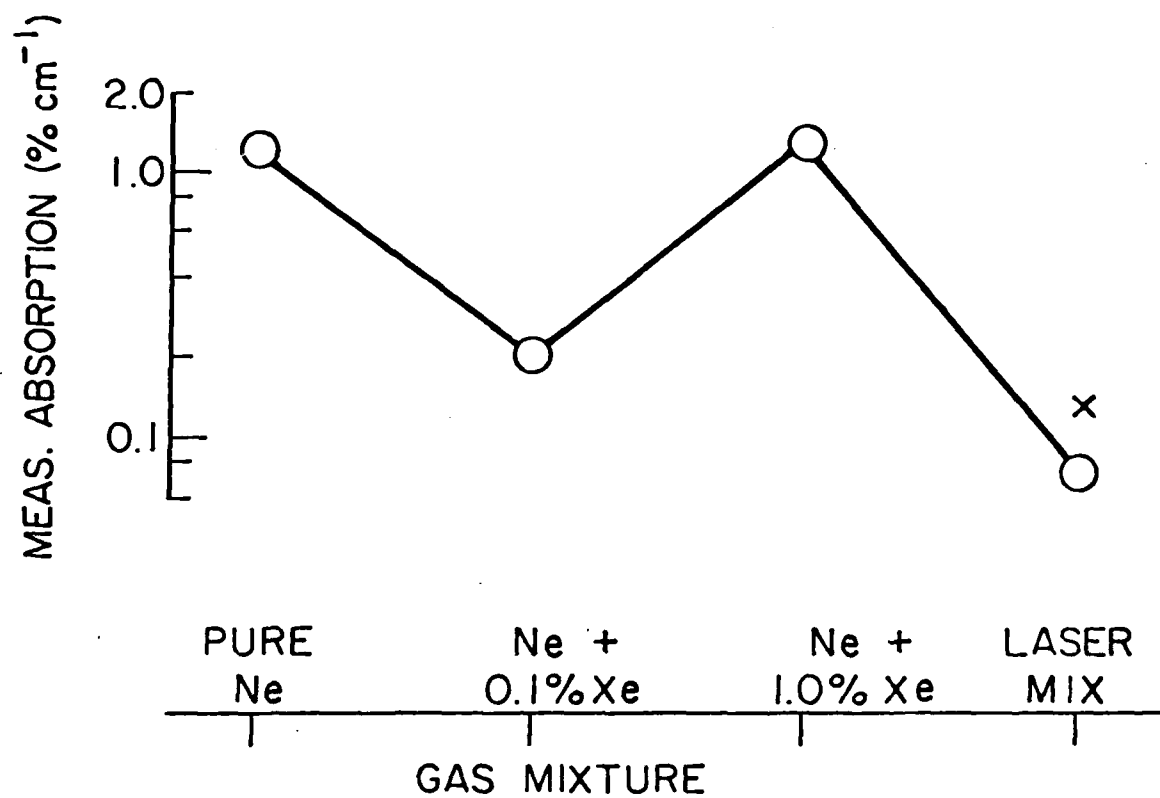


Fig. 3

The Role of the C State in the XeF Laser

T. G. Finn,[†] L. J. Palumbo, L. F. Champagne
Laser Physics Branch
Optical Sciences Division
Naval Research Laboratory
Washington, D. C. 20375

Ne/Xe/NF₃ mixtures were irradiated by a cold cathode e-beam, and the fluorescence yields of the B- and C-states of XeF were measured as a function of neon pressure from 200 to 5300 torr. At low neon pressures, the fluorescence yield of the B-state corresponds to one photon emitted for each neon ion formed. As the neon pressure is increased the fluorescence yield of the B-state decreases, but the ratio of the C emission to B emission approaches unity. If the C is formed through a channel which is independent of the B-state, then the ultimate efficiency of the XeF laser is severely limited. However, analysis of the data with a XeF kinetics model indicates that the enhanced C emission results from two-body quenching of the B-state by neon. We conclude that the XeF laser performance has been limited by other processes, namely incomplete vibrational relaxation and ground state bottlenecking.

[†]Science Applications, Inc., Arlington, VA. 22202

INTRODUCTION

XeF is the second rare gas monohalide laser system (after KrF) to demonstrate high efficiency and output power. Initially, the XeF laser was operated in an argon diluent but its efficiency was well below one percent because of transient absorption in the medium. Champagne and Harris found a significant improvement in the output power and efficiency with neon as the diluent.⁽¹⁾ This work showed that the transient absorption present in pure neon, although comparable to that in pure argon, was markedly reduced by the addition of a small amount of xenon. Previously, we developed a computer model which simulates the kinetics in an electron e-beam pumped XeF laser. Analysis with the model has shown that the addition of a small amount of xenon to pure neon significantly reduces the concentration of neutral species such as Ne^* and Ne_2^* through the mechanisms of Penning and associative ionization, but only slightly diminishes the concentration of charged species.⁽²⁾ Consequently, we have attributed the transient absorption in pure neon to the neutral species.

XeF has two intense emission features, the B \rightarrow X system around 351 nm, and the broad C \rightarrow A system centered around 460 nm. Our kinetic model predicts that the formation efficiency of XeF^* is high, but it cannot determine which states (B or C) are populated. Recently Kligler et al.⁽³⁾ have shown that the C-state of XeF lies 700 cm^{-1} below the B-state, and that the emission intensity of both states are equal under pumping conditions similar to those in the laser. The importance

of the latter result is the following: --if the C-state is formed in such a way that its excitation energy is not channeled through the B-state, then almost half the total excitation is lost. Thus, the maximum efficiency of the XeF laser would be approximately five percent, which is the value recently obtained by heating the mixture.^(4,5) If, on the other hand, the C-state is formed through the B-state then all the excitation present in the C-state is potentially extractable as laser radiation. To resolve this question, and to characterize further the XeF laser, we have investigated the fluorescence from the B- and C-states and analyzed the results with a computer model.

EXPERIMENTAL

The apparatus used in these experiments has been described previously and will be reviewed briefly.⁽⁶⁾ The kinetics chamber is made from aluminum and has an active volume of $1.5 \times 1 \times 20 \text{ cm}^3$. The chamber is mounted directly to the electron gun vacuum chamber with a thin titanium foil separating the two. The cold-cathode electron gun produces a beam of 280 KeV electrons with a pulse duration of $\sim 1 \text{ } \mu\text{sec}$. The peak current density into the laser gas is 2 A/cm^2 . Fluorescence is observed perpendicular or parallel to the electron beam direction with calibrated photodiodes and filters. All the kinetics experiments used concentrations of six torr Xe and 2 torr NF_3 , which are the values corresponding to the optimum laser mixture. The dominant kinetic processes have characteristic times which are much shorter than the pulse duration, thus the excited and ionic species are in quasi-equilibrium.

RESULTS

In Figure 1, the XeF ($B \rightarrow X$) and ($C \rightarrow A$) fluorescence from a mixture of Ne/Xe/NF₃ is given as a function of neon pressure. At low neon pressure the ratio of $B \rightarrow X$ to $C \rightarrow A$ emission intensity is approximately three to one. As the neon pressure increases, the fluorescence from both states increases but at high pressures the $B \rightarrow X$ fluorescence begins to level off while the C fluorescence continues to rise. At the optimum laser mixture (five atmospheres) the $C \rightarrow A$ emission is over seventy percent of the $B \rightarrow X$ emission.

More information about the B and C states can be obtained by calculating their corresponding fluorescence yields. The fluorescence yield is defined here as the ratio of the number of photons emitted from a state divided by the number of ion-electron pairs produced by the electron beam. A fluorescence yield of one corresponds to one photon emitted for each ion formed. It is possible for the total fluorescence yield to be greater than unity. For each one hundred ions that are created, the electron beam also produces about thirty excited neutral atoms which can lead to the upper laser level.⁽⁷⁾

Relative fluorescence yields can be put on an absolute basis by normalizing to the absolute fluorescence yield of the N₂ second positive system produced in mixtures of argon with five percent nitrogen. At a total pressure of two atmospheres, Huestis and Tang have determined the fluorescence yield of the second positive system to be approximately nine percent over the e-beam current range of 1-10 A/cm² incident to the active volume.⁽⁸⁾ Using the argon/nitrogen fluorescence as a secondary standard,

we obtained the absolute fluorescence yield of the XeF ($B \rightarrow X$) and ($C \rightarrow A$) transitions as a function of neon pressure. Since the thickness of the target gas is small compared to the penetration depth of the e-beam, the number of ions produced is linearly proportional to the gas pressure. Thus, the relative fluorescence yield is equal to the signal intensity divided by the neon pressure.

In Figure 2 the inverse of the absolute fluorescence yield for the XeF transitions ($B \rightarrow X$) and ($C \rightarrow A$) is plotted versus neon pressure. This method of data analysis is similar to a Stern-Volmer plot and is useful in interpreting the data. Moreover, the fluorescence yields have been corrected to account for quenching by Xe and NF_3 . This correction, which is largest in the low pressure region, is about ten percent. As can be seen in the figure, at low neon pressure the fluorescence yield of the $B \rightarrow X$ transition approaches unity which corresponds to a fluorescence energy efficiency of ten percent. However, as the neon pressure is increased the fluorescence yield decreases so that at the optimum laser mix of five atmospheres it is approximately 0.3. Meanwhile, the fluorescence yield of the $C \rightarrow A$ transition varies slowly and approaches 0.25 at zero pressure. There are two likely explanations for the pressure behavior of the fluorescence yields. First, at high pressure the formation efficiency of the B-state is close to unity, but the state is quenched to the C-state which lies 700 cm^{-1} below it. Second, at high pressure, the excitation energy is intercepted before it reaches the B-state and channeled directly into the C-state. In the former case, almost all of the excitation can be considered as potential laser

radiation because the energy can be extracted from the B-state before it is quenched to the C-state. However, in the latter case, the energy is directly pumped into the C-state and is virtually inaccessible. Thus, the manner in which the C-state is formed at high pressure determines the ultimate efficiency of the laser.

DISCUSSION

The C-state can be formed in three ways: direct excitation, quenching from B to C by neutral species, and quenching from B to C by electrons. Our data indicates that electron mixing of the B and C states is not significant up to a pumping rate of 7 A/cm^2 . This conclusion is based on the following results. First, as the NF_3 concentration in the kinetics chamber was varied from two to one hundred torr, we observed only a ten percent decrease in the B/C emission ratio. Since the removal rate of the electrons, and thus their equilibrium concentration, is determined by the concentration of the attaching species, NF_3 , the electron density varied greatly but the B to C ratio remained approximately constant. Furthermore, other experiments were conducted in the laser mixture (5 atm) with 7 A/cm^2 e-beam pumping current and the B to C ratio was found to be the same as in the kinetics experiments with 2 A/cm^2 pumping rate. Finally, if electron mixing were significant the B/C emission ratio should be much higher than is observed. The separation of the B and C states is 700 cm^{-1} which is about .08 eV. If the electron temperature were 1eV, the states would be approximately equally populated. Since the ratio of transition probabilities for the

B and C states is approximately seven, the B to C emission ratio would be much greater than one.⁽⁹⁾ Instead the observed emission ratio extrapolates at high pressure to a value of 0.6 which corresponds to a temperature of .035 eV, close to the temperature of the background gas. Thus, electron mixing is not important in determining the ratio of the B and C states and a model based solely on neutral kinetics may be used.

The neutral kinetics model must include direct pumping to B and C, quenching from B to C and the reverse reactions, and quenching from B and C to products. For direct pumping the absolute fluorescence yields extrapolated to zero pressure were used. The quenching rate constants used in the model are given in Table I. The applicability of the rates will be discussed later. The predictions of the model based on absolute fluorescence yields and quenching by neutrals are given as the solid lines in Figure 1. As can be seen from the figure, the model is in good agreement with the data. Quenching of the B-state, primarily through two-body collisions with neon, accounts for all the observed decrease in the fluorescence yield as the neon pressure is increased. If significant interception of the B-state were present, the model values would be much higher than the observed B emission. Moreover, if at high pressure a larger fraction of the excitation were channeled directly into the C-state, the model predictions for the C emission would be much less than the observed values. Initially, however, the predicted C emission was higher than the observed value indicating that some quenching of the C-state by the background gas occurs. The C-state quenching rate which fits the data is given in Table I.

Three important conclusions can immediately be drawn from the model analysis. First, almost eighty percent of the ions and electronically excited neutrals formed channel their excitation directly into the B-state. Second, the back reaction, C to B, is small such that once the energy is in the C state it is virtually lost. Third, the enhanced C emission at high pressure is due to quenching from B to C primarily through two body collisions with neon. In fact, two-thirds of the C population results from the B-state. The last conclusion has been verified experimentally. Since a large fraction of the C-state population results from the B-state, the C emission rate will decrease if the steady state B population is decreased as occurs in a saturating laser field. The depression of the C emission in a saturating laser field has been observed.⁽¹⁰⁾

The accuracy of the model predictions depends on the reliability of the rate constants used. Over fifty percent of the B-state quenching is due to two body neon quenching, a process whose rate constant and branching are well characterized.⁽¹¹⁾⁽¹²⁾ However, forty percent of the quenching is due to three body neon and neon plus xenon reactions. The rate constants for these processes have been derived from electron-beam pumped mixtures, and, strictly speaking, the rates could correspond to interception rather than quenching processes. That is, these reactions could channel excitation away from the B-state rather than quench the B-state. In order to characterize the XeF laser precisely the quenching rate constants and branching ratios for these processes have to be known.

Assuming the reliability of the quenching rate constants, we can summarize the results and conclusions:

(a) The formation efficiency of the B-state is approximately one XeF (B) molecule formed for each ion pair created.

(b) The decrease in the B-state fluorescence yield observed at high pressure is due to quenching, primarily through two body collisions with neon.

(c) The enhanced C emission observed at high pressure is due to quenching from B to C rather than interception of the B-state.

(d) Since the formation efficiency of XeF(B) is high, other processes are limiting the laser performance. Most likely, these processes are incomplete vibrational relaxation and bottlenecking of the state due to finite relaxation rates.

The authors wish to thank W. T. Whitney for lending us his electron beam apparatus, D. Shores for his technical assistance, and D. Huestis, SRI, and K. Tang, Maxwell Labs. Inc., for making available to us their unpublished data.

TABLE I

<u>Quenching Reaction</u>	<u>Rate Constant</u>	<u>Branching Ratio to XeF (C)</u>	<u>Reference</u>
XeF (B) + Ne	$7.7 \times 10^{-13} \text{ cm}^3/\text{sec}$.95	a, b
+ 2Ne	$2.7 \times 10^{-31} \text{ cm}^6/\text{sec}$.5*	c
+ Ne + Xe	$8.3 \times 10^{-31} \text{ cm}^6/\text{sec}$.5*	c
+ Xe	$1.1 \times 10^{-10} \text{ cm}^3/\text{sec}$.45	b
+ NF ₃	$8.4 \times 10^{-11} \text{ cm}^3/\text{sec}$.64	a, b
XeF (C) + Ne + Xe	$4.0 \times 10^{-31} \text{ cm}^6/\text{sec}$	products	this work

* assumed for model calculations.

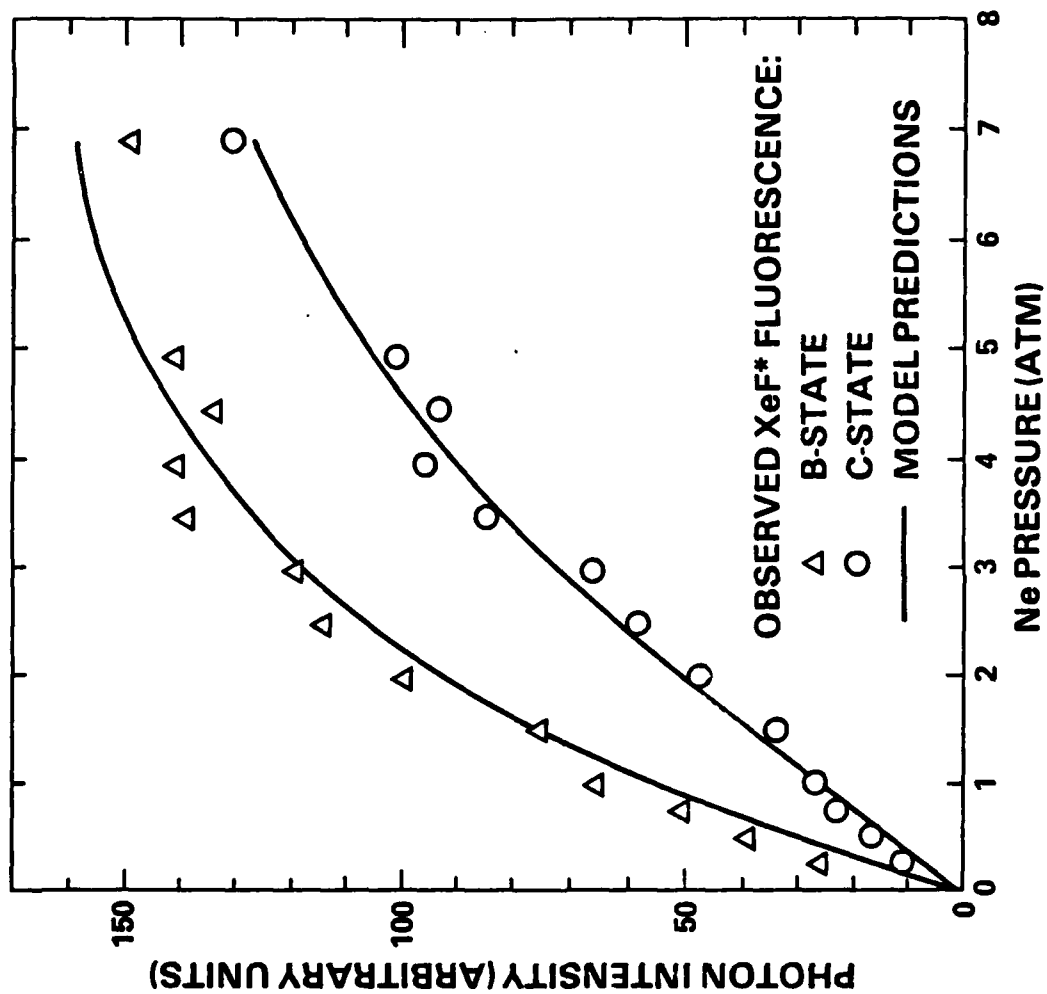
a - ref 10
b - ref 11
c - ref 12

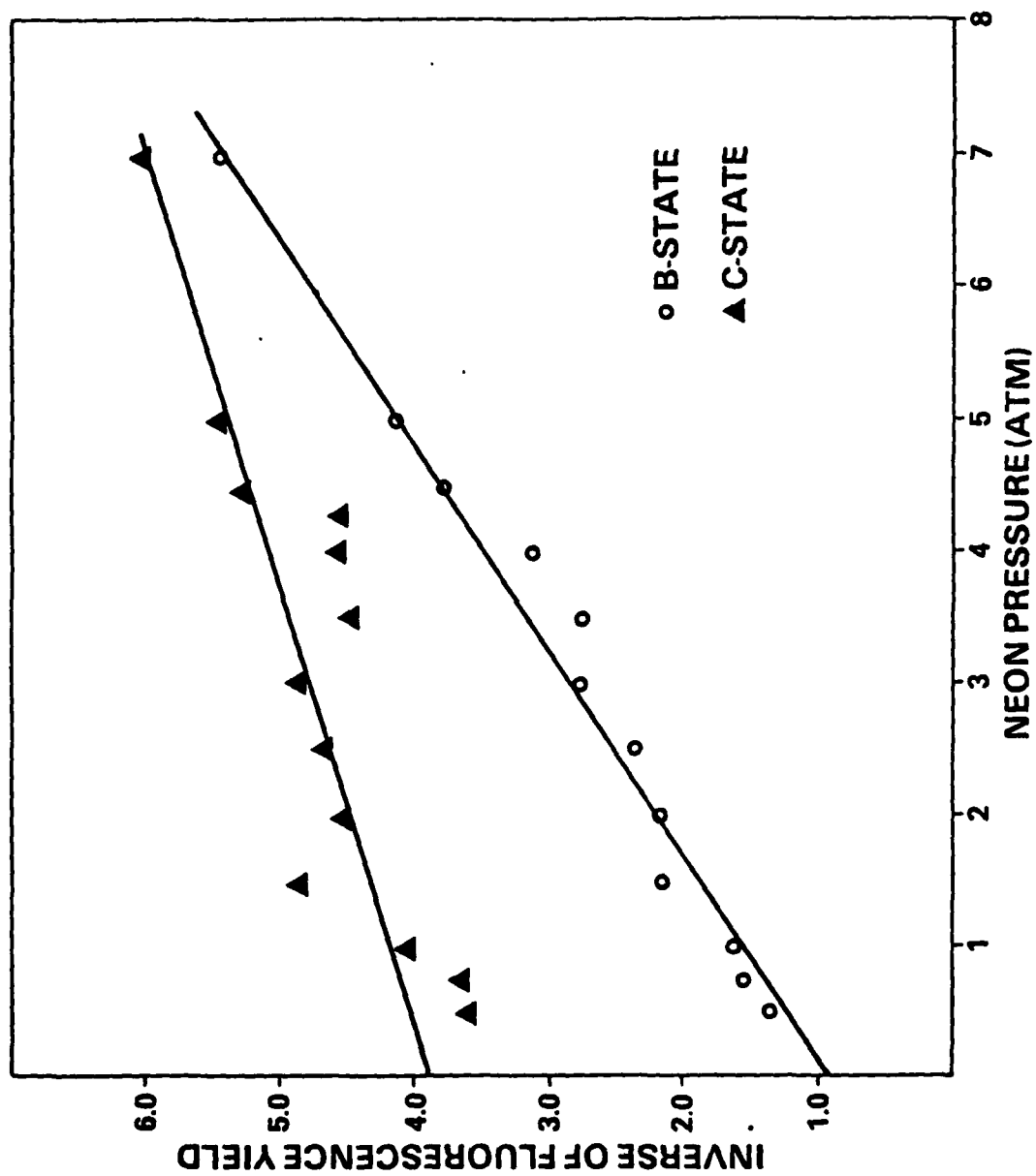
REFERENCES

1. L. F. Champagne and N. W. Harris, Appl. Phys. Lett. 31, 513 (1977).
2. T. G. Finn, L. J. Palumbo and L. F. Champagne, Appl. Phys. Lett. 33, 148 (1978).
3. D. Kligler, H. H. Nakano, D. L. Huestis, W. K. Bischel, R. M. Hill and C. K. Rhodes, Appl. Phys. Lett. 33, 39 (1978).
4. L. F. Champagne, private communication.
5. J. Hsia, to be published.
6. N. W. Harris, F. O'Neill and W. T. Whitney, Appl. Phys. Lett. 25, 148 (1974).
7. L. R. Peterson and J. E. Allen, Jr., J. Chem. Phys. 56, 6068 (1972).
8. D. L. Huestis, R. M. Hill, D. J. Eckstrom, M. V. McCusker, D. C. Lorents, H. H. Nakano, B. E. Perry, J. A. Margevicius and N. E. Schlotter, Report No. MP 78-07, Stanford Research Institute International, Menlo Park, CA (May, 1978).
9. J. G. Eden and R. W. Waynant, J. Quantum Electronics (to be published).
10. L. F. Champagne, unpublished.
11. J. G. Eden and R. W. Waynant, Optics Letters 2, 13 (1978).
12. H. C. Brashears, Jr., and D. W. Setser, Appl. Phys. Lett. (to be published).
13. M. Rokni, J. H. Jacob, J. A. Mangano and R. Brocher, Appl. Phys. Lett. 32, 223 (1978).

FIGURE CAPTIONS

- Figure 1. Observed fluorescence of XeF B- and C-states with 6 torr Xe and 2 torr NF_3 as a function of neon pressure. The solid lines are the model calculations based on the formation efficiency and quenching rates given in the text.
- Figure 2. Inverse of the fluorescence yields of the XeF (B \rightarrow X) and (C \rightarrow A) emissions as a function of neon pressure. For the B-state the zero pressure intercept of unity indicates that its formation efficiency is approximately one XeF (B) molecule for each neon ion formed.





memorandum

DATE: 17 January 1979

REPLY TO
ATTN OF: 5540-52:TGF/LJP:rmbSUBJECT: Depletion of the halogen donor in the XeF Laser
ENCL : (1) Figure 1

TO: S. K. Searles

1. This memo is in response to your directive to investigate depletion of the halogen donor in e-beam pumped XeF lasers. It is the purpose of this investigation to determine the extent of NF_3 depletion in the laser mixture, to characterize its effects on laser performance, and to estimate under what conditions these effects are significant.

2. Using our kinetics model, we have calculated the extent of depletion and its possible consequences in the optimal laser mix (4 atm Ne/12 torr Xe/6 torr NF_3) for pumping currents of 10 A/cm², pulse lengths of 1 and 10 μsec , and operation at elevated temperatures.

3. The major model predictions are the following:

a) almost 25% of the NF_3 is depleted after 1 μsec , however, the effect on laser output is not significant.

b) the major effects of depletion are likely to be an increase in the absorption due to Xe_2^+ , and greater formation through the Xe^+ - neutral channel.

c) for 10 μsec operation, the consequences and extent of depletion depend on the electron attachment rates and the termolecular recombination rates of the depletion products, NF_2 , NF and F .

4. Background

Efficient operation of the XeF laser has been achieved in neon diluent for pulse durations of approximately 1 μsec , and with energy loadings of less than 200 J/l. In order to project the laser performance at longer pulses with loadings of significantly more energy, one must determine what new effects will occur under these conditions and assess their impact.

Two effects which are small for 1 μsec operation but significant for longer pulses are depletion of the halogen donor, NF_3 , and gas heating from pump energy deposition. Depletion of the halogen donor can effect several aspects of the laser: the formation chain, absorption, quenching and interception. In the XeF laser, quenching and interception by NF_3 have only a small effect on the laser output. However, NF_3 , which produces F^- by dissociative attachment, controls the ion balance in the laser plasma, which in turn, controls the dominant formation and absorption processes. Thus, depletion of NF_3 may decrease the efficiency of the formation and extraction processes. Consequently, in this memo we



Buy U.S. Savings Bonds Regularly on the Payroll Savings Plan

U.S. Government Printing Office: 1976-241 529/3818

OPTIONAL FORM NO. 10
(REV. 7-76)
GSA FPMR (41 CFR) 101-11.6
5010-112

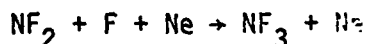
have addressed depletion as it affects the ion balance in the laser plasma. However, we estimate that a temperature rise of a few hundred $^{\circ}\text{K}$ will occur for long pulses due to e-beam energy deposition. Recent results on heated XeF indicate that the laser performance decreases above a certain temperature (1). If the laser works well only in a narrow temperature range, then for long pulse operation, the performance may be adversely affected by the amount of energy deposited by the e-beam.

5. Approach

For the model simulation, the optimum laser mixture at 10 A/cm^2 pumping rate obtained by Rokni et al. (2) was used. This mixture is 4 atm neon, 12 torr xenon and 6 torr NF_3 . The pumping pulse duration was varied from 1 μsec to 10 μsec . Simulations were run varying the attachment rates and recombination rates of the depletion products. The effect of elevated temperature was crudely approximated by the following assumptions: first, the XeF ground state removal rate was significantly increased, (3) second, the absorption cross section at the laser wavelength of Xe_2^+ was reduced (4) so that greater amounts of xenon could be added to the mixture (5), and third, vibrational relaxation of the XeF (B) state manifold was increased (1).

6. Extent of Depletion

The extent of depletion of NF_3 is determined by the balance between the removal and reformation processes. Dissociative attachment of electrons is the dominant depletion process. The major replenishment process is three-body recombination of the depletion products, i.e.,



If the recombination rate is insignificant then ~ 15% of the NF_3 will be depleted in the first microsecond. Moreover, 90% will be depleted in 3.5 μsec . However, if the three-body recombination rate is 10^{-31} the NF_3 concentration will stabilize at more than half its initial value.

7. Effects of Depletion

The most serious effect of depletion will be to decrease the concentration of F^- , a key species in both the formation and extraction processes. In the ion formation chain, which accounts for almost 90% of the XeF(B) production during the first microsecond of the pulse, F^- recombines with various xenon ion complexes to form the upper laser level. Furthermore, by recombining with Xe_2^+ , F^- removes it as a major absorption species. The principal effect of F^- depletion will be to increase the absorption

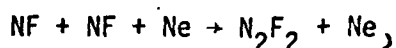
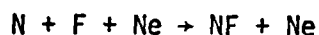
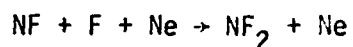
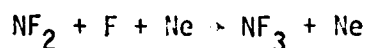
due to Xe_2^+ . Another effect will be to shift the formation process from one completely dominated by ion-ion recombination reactions to one in which excited-neutral reactions are of comparable importance. Although ion-ion recombinations form the XeF (B) state with 80% efficiency (6), reactions of Xe^* with NF_2 or NF may not be nearly as efficient. Thus the formation efficiency may decrease as well as the extraction efficiency.

Other possible harmful effects of depletion involve the depletion products themselves. Interception or quenching by the NF_2 , NF or F could be significant if the corresponding rate constant were of the order 10^{-9} . As a final point, it has been recently pointed out to us that NF_2 does not absorb at 350 nm, but NF might.

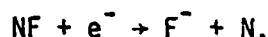
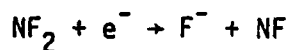
8. Assessment of Depletion Effects

We have assessed the extent and effect of NF_3 depletion over the range where the three-body recombination rate constant of the depletion products is varied from 10^{-34} to 10^{-30} cm^6/sec , and their attachment rate constant is varied from 10^{-10} to 5×10^{-9} cm^3/sec . In general, the extent of depletion depends primarily on the termolecular recombination rate, and the consequences depend mainly on the attachment rate of the depletion products. If the recombination rate constant is greater than 10^{-31} cm^6/sec , the NF_3 is reformed so rapidly that depletion is not significant. Likewise, if the electron attachment rate constant is the same as that of NF_3 (5×10^{-9} cm^3/sec), the F^- concentration does not drop and the laser performance is unaffected. In order to avoid complications resulting from the XeF ground state and incomplete vibrational relaxation, we have calculated laser performance under "heated" conditions with various attachment and recombination rates for the depletion products. "Heated" conditions were approximated by the following: (1) the XeF ground state was assumed to be unbound, (2) the absorption cross section at the laser wavelength of Xe_2^+ was set at half the room temperature value and the concentration of xenon increased to 1.5 times the room temperature value, (3) the relaxation time for vibrational mixing of the B-state manifold was set at 1 nsec. Moreover, it was assumed that neutral reactions involving Xe^* and the depletion products NF_2 and NF did not branch to the B-state.

Selected results of the calculations for heated XeF are summarized in Figure 1. The computed laser output energy for a 10 μsec pump pulse is plotted in this figure as a function of k_{rec} , for various values of the electron attachment rate coefficient, β . Here, k_{rec} is the rate constant for the following termolecular recombination reactions,



and β is the rate constant for



Other relevant attachment and recombination rates were obtained from the literature.

The important conclusions from Figure 1 are:

a) the laser performance will not degrade if the attachment rate constant of the depletion products is approximately $5 \times 10^{-9} \text{ cm}^3/\text{sec}$, or if the three-body recombination rate is at least $1 \times 10^{-31} \text{ cm}^6/\text{sec}$.

b) the laser performance will degrade only 10% if the attachment rate constant is at least $5 \times 10^{-10} \text{ cm}^3/\text{sec}$ and the recombination rate is at least $1 \times 10^{-32} \text{ cm}^6/\text{sec}$.

9. Summary

We can draw the following conclusions:

a) the extent of depletion depends primarily on the termolecular recombination rate which controls the NF_3 reformation.

b) the effect of depletion depends on the electron attachment rate of the depletion products which controls the F^- production.

c) the first major effect of depletion will be increased absorption due to Xe_2^+ .

d) the second major effect will be increased formation through Xe^* neutral reactions, however, the total formation rate will remain approximately constant.

e) effects of depletion on laser performance range from negligible to significant depending on the recombination and attachment rates.

10. Recommendations

As a result of this study we recommend that the following quantities are necessary to determine the effect of depletion on the laser performance:

a) electron attachment and termolecular recombination rate constants for NF_2 and NF .

b) the rate constants and branching ratios for reactions of Xe^* , and F^* with NF_2 and NF .

In addition, the following quantities are also important:

a) rate constants for NF_2 and NF quenching of XeF^* and F_2^* .

b) photoabsorption properties of NF .

Thomas Finn
T. G. Finn

L. J. Palumbo
L. J. Palumbo
Laser Physics Branch
Optical Sciences Division

References

1. J. Hsia, et al., to be published in Appl. Phys. Lett. (15 Dec 1978).
2. M. Rokni, J. H. Jacob, J. A. Mangano, J. Hsia, and A. Hawryluk, Papers CA-2, CA-3, and CA-4, 30th Annual Gaseous Electronics Conference, Palo Alto, CA. (18 Oct 1977).
3. T. G. Finn, L. J. Palumbo, and L. F. Champagne, Appl. Phys. Lett. 33, 148 (15 July 1978).
4. W. Wadt, D. C. Cartwright, and J. S. Cohen, Appl. Phys. Lett. 31, 673 (1977).
5. L. F. Champagne, private communication.
6. T. G. Finn, L. J. Palumbo, and L. F. Champagne; to be published in Appl. Phys. Lett. (1 Jan 1979).

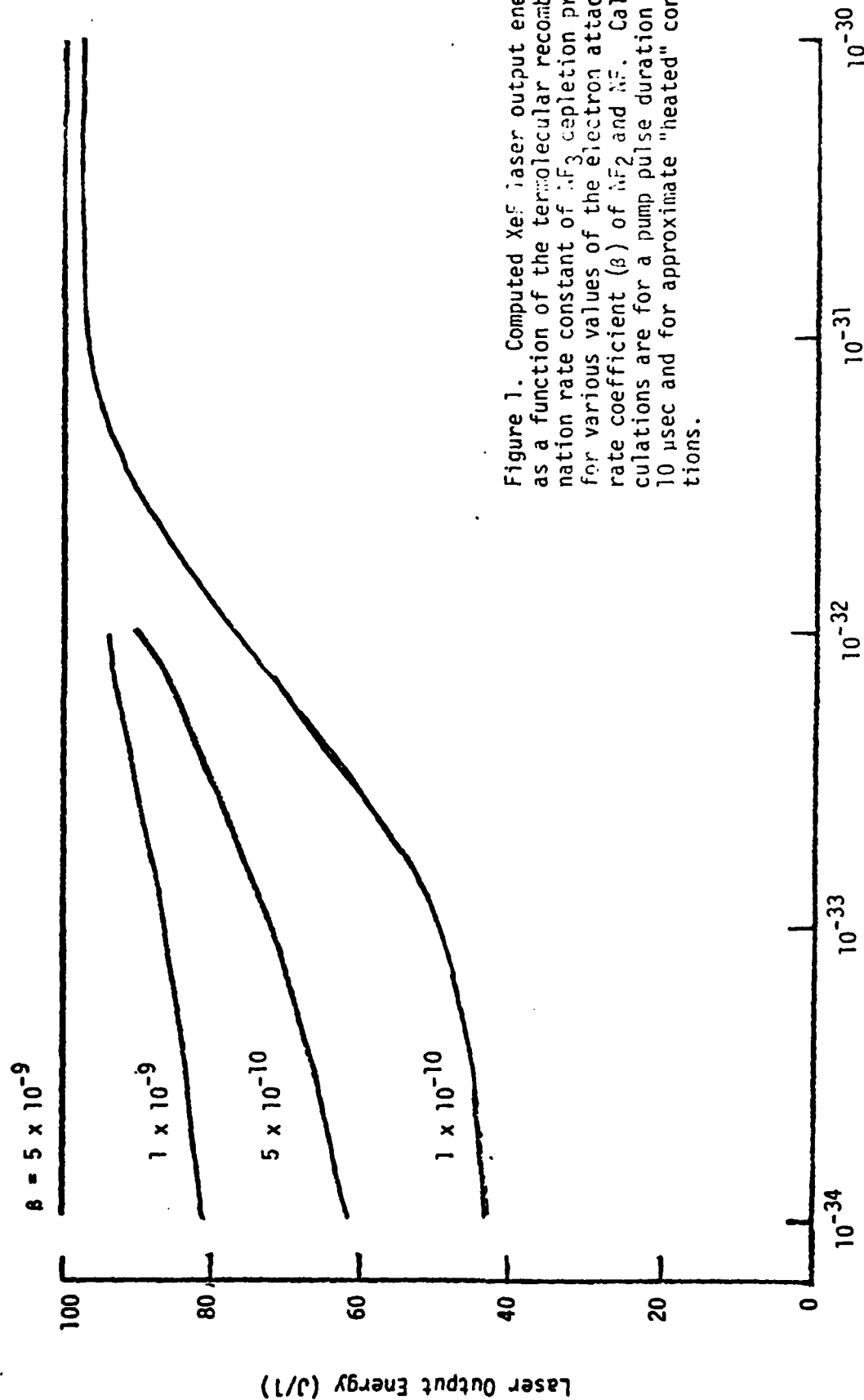


Figure 1. Computed XeF laser output energy as a function of the termolecular recombination rate constant of XeF_3 depletion products for various values of the electron attachment rate coefficient (β) of XeF_2 and XeF . Calculations are for a pump pulse duration of 10 μsec and for approximate "heated" conditions.

Termolecular Recombination Rate (cm⁶/sec)

